SHORT THESIS FOR THE DEGREE OF DOCTOR OF PHILOSOPHY (PHD)

The effects of CBA and ABT-333 on the mammalian ventricular action potential and its ionic currents

by Csaba Bálint Dienes, Pharm.D.

Supervisor: Norbert Szentandrássy, MD, PhD

UNIVERSITY OF DEBRECEN
DOCTORAL SCHOOL OF MOLECULAR MEDICINE

DEBRECEN, 2024

The effects of CBA and ABT-333 on the mammalian ventricular action potential and its ionic currents

By Csaba Bálint Dienes, Pharm.D.

Supervisor: Norbert Szentandrássy, MD, PhD.

Doctoral School of Molecular Medicine, University of Debrecen

Head of the **Defense Committee**:	László Virág, PhD, DSc
Reviewers:	András Farkas, PhD
	Péter Béla Hajdu, PhD
Members of the Defense Committee:	Gábor Czirják, PhD, DSc
	Béla Juhász, PhD

The PhD Defense takes place at the
Lecture Hall of Bldg. A, Department of Internal Medicine, Faculty of Medicine,
University of Debrecen at 13:00, on 11th April 2024

1. Introduction

TRPM4 is a member of the melastatin subfamily of the Transient Receptor Potential channel family. Its expression has been detected in several human organs. It is involved, among others, in the regulation of membrane potential and Ca^{2+} homeostasis in cells of both excitable and non-excitable tissues, insulin secretion, immune response, tumorigenesis and cerebral vasoconstriction.

In the heart, TRPM4 channels are detected in both myocytes and the cardiac conduction system. Mutations in TRPM4 channels in the heart can lead to conduction defects and TRPM4 is thought to be involved in myocardial hypertrophy and ischemia-reperfusion injury.

So far, the physiological and pathophysiological functions of TRPM4 have been investigated either in knock-out animal models or by pharmacological approaches with inhibitors of the channel, including 9-phenanthrol, glibenclamide or flufenamic acid. Unfortunately, none of these compounds are sufficiently selective. However, for functional studies of the channel, a selective agent or at least a combination of available TRPM4-modulator agents with appropriate complementary pharmacological agents would be needed. The latter approach however requires great care.

In my work, I present the effects of a drug developed specifically to inhibit the TRPM4 channel, CBA, on myocardial cells in the left ventricle of dogs. CBA is thought to be a potentially selective TRPM4 inhibitor, however, before using it for TRPM4 functional assays, our working group performed selectivity assays with CBA to see if CBA affects any main current of the ventricular myocardial action potential (AP) and to evaluate the CBA action on AP morphology. In addition, we also investigated TRPM4 channel expression in a collaborative work, the results of which are also presented.

The delayed rectifier potassium current plays a primary role in the repolarization of ventricular myocytes. In ventricular myocytes, two components have been described: the fast component (I_{Kr}) is responsible for phase 3 repolarization of the AP, whereas the slow component (I_{Ks}) is a member of the so-called repolarization reserve. The latter means that I_{Ks} is not involved in normal repolarization but ensures repolarization when it is increased during a prolonged AP. Decreased I_{Kr} current leads to long QT syndrome and early

afterdepolarisation (EAD), and therefore can cause potentially life-threatening arrhythmias and sudden cardiac death.

Several selective inhibitors of I_{Kr} are known, such as dofetilide or E-4031. Both compounds contain a methanesulfonamide group in their chemical structure and also significantly increase the duration of ventricular AP.

ABT-333 (dasabuvir) is an antiviral agent used in the treatment of hepatitis C. The molecule, like some inhibitors of hERG channels responsible for the formation of I_{Kr} (such as dofetilide and E-4031), contains a methanesulfonamide group. Based on this similarity, ABT-333 also has potential I_{Kr} inhibitory activity, but the effects of the compound on the ventricular myocardium are not yet known. In my work, I will present the effects of ABT-333 on the AP morphology of canine ventricular myocardial cells and its underlying effects on ionic currents. Thanks to our collaboration partners, the effects of ABT-333 on hERG channels have also been investigated in expressed cells, and the results are also presented.

2. Aims

Based on the so far known role of TRPM4 in the heart the first aim of our research was

- to prove the expression of TRPM4 protein.

We wanted to explore the actions of a new compound (CBA) directly developed as TRPM4 inhibitor on:

- the morphology of cardiac action potential
- the short-term variability of repolarization.

To investigate the channel functionally, we need a selective inhibitor, so we first perform selectivity assays with the compounds to see if those affect ion channels other than TRPM4, therefore we tested

- the CBA-sensitive current with action potential voltage clamp (APVC) technique,
- the action of CBA on repolarizing currents.

Based on the chemical structure of ABT-333, the molecule has the potential to inhibit one of the major repolarizing currents (I_{Kr}), but the effect of this agent on ventricular AP is unknown. Therefore, we wished to investigate:

- the action of 1 µM ABT-333 on left ventricular AP of the canine heart,
- concentration-dependent actions of ABT-333 on various AP parameters,
- the ABT-333-sensitive current with APVC technique,
- and last but not least the action of ABT-333 on the ionic current of expressed hERG channels.

Of course, it is not easy to obtain cells from healthy human hearts for experimental purposes, so for our experiments we isolated left ventricular myocytes from canine hearts, which are electrophysiologically one of the best models of human myocardial cells.

3. Materials and methods

3.1. Isolation of Ventricular Myocytes

Our experiments were carried out on myocardial cells enzymatically isolated from the left ventricle of the heart of mixed sex and breed, 1-3 years old adult dogs bred specifically for experimental purposes. The anterograde segment perfusion technique was used to isolate myocardial cells with a protocol in line with the ethical standards laid down in the Declaration of Helsinki in 1964 and its later amendments as well as with the Guide to the Care and Use of Experimental Animals (US NIH publication number 85-23, revised 1996). The experimental protocol was also approved by the Institutional Animal Care (licence No.: 9/2015/DEMÁB).

3.2. Recording of Action Potentials

The APs were triggered by an electronic stimulator with current pulses of 120-130% of the stimulus threshold and measured using conventional microelectrode technique. The APs were digitized, evaluated, the following parameters were determined in ten consecutive APs then averaged: APD_{50}, APD_{75} and APD_{90} (duration of the AP from the peak to 50, 75 and 90% of repolarization, respectively), maximal rate of phase 0, 1, and 3 (V^{+}_{max} , V_{Ph1}max and V^{-}_{max}, respectively), resting membrane potential (RMP), overshoot potential (OSP), APA (action potential amplitude determined as the difference between OSP and RMP), $Plateau_{20}$ and $Plateau_{50}$ amplitude (the difference between the resting membrane potential and the membrane potential values measured at 20% and 50% of the time to 90% repolarization, respectively) and the membrane potential at the half duration of APD_{90} ($Plateau_{50}$).

3.3. Analysis of the action potential repolarization variability

A series of 50 consecutive action potentials were recorded and analysed offline to calculate the short-term variability of repolarization (SV) using the following formula:

$$SV = \frac{\sum_{n=1}^{i}(|APD_{n+1} - APD_n|)}{i\sqrt{2}}$$

where SV is the short-term variability, APD_n and APD_{n+1} indicate the APD_{90} values of the *n*th and (*n* + 1)th APs, respectively, and *i* denotes the number of consecutive beats analyzed. As the value of SV strongly depends on the value of APD_{90}, SV can be best judged as a function of APD. To further analyzed repolarization variability, the differences between consecutive APD_{90} values were grouped in ranges (below 20 ms in 1 ms ranges and above 20

ms differences and 5 ms ranges) and the overall probability of their appearance was calculated in each cell.

3.4. Voltage-Clamp Studies

Membrane currents were recorded using the patch-clamp technique in whole-cell configuration. Our experiments were performed using conventional voltage-clamp and action potential voltage-clamp (APVC) techniques. In conventional voltage-clamp experiments, the ion channel under investigation was excited by square pulses while the other ion channels were inhibited. In the action potential voltage-clamp experiments, cells were stimulated with a so-called "canonical" AP instead of square pulses, which is a typical AP previously recorded on a midmyocardial cell. In cells stimulated in this way, all the ionic currents under the AP that are affected by the compound of interest can be examined together. CBA- or ABT-333-sensitive currents were obtained by pharmacological subtraction: the current signals recorded at the end of 5 min 10 µM CBA or 15 min 10 µM ABT-333 perfusion were subtracted from the signals measured in control (physiological Tyrode's solution). Cells were perfused again with physiological Tyrode solution (washout) for 5 min after CBA or 20 min for ABT-333.

3.5. Recording of hERG Currents

Whole-cell currents of voltage-clamped HEK (human embryonic kidney) cells stably expressing hERG channels were recorded by manual patch-clamp technique. The effect of 1, 3, 10 and 30 µM ABT-333 on the gating (activation, inactivation, deactivation) of hERG channels was studied by applying corresponding square pulses at room temperature (20-24°C).

3.6. Protein Sample Preparation and Western Blot Analysis

For Western blot experiments, total cell lysates were prepared from canine left ventricular cardiomyocytes and from tissue samples (excised from the wall of the four chambers of the heart) by mechanical force methods. Protein concentrations were determined by BCA (Bicinchoninic acid) protein assay, and samples were subjected to SDS-PAGE (Sodium Dodecyl Sulfate-Polyacrylamide Gel Electrophoresis) and transferred to nitrocellulose membranes. Membranes were blocked with 5% dry milk-PBS (Phosphate

Buffered Saline) solution and incubated with anti-TRPM4 and anti-α-actinin primary antibodies followed by HRP-conjugated secondary antibody labeling. The background corrected optical density of the bands determined by TRPM4-specific chemiluminescence was determined by densitometry using ImageJ program and normalized to the optical density of the α-actinin specific band of the samples.

3.7. Statistical analysis

All values are presented as arithmetic mean ± Standard Error of the Mean (SEM). Given the biological variability among cells, each cell was treated as independent in the statistical tests, although more than one cell could be obtained from the same animal. Statistical significance of differences was evaluated using one-way ANOVA followed by Student's t-test. Differences were considered significant when $p < 0.05$.

4. Results

4.1. Expression of TRPM4 Protein

For protein expression studies, tissue samples and left ventricular isolated cells were obtained from five animals. Protein separation with electrophoresis and the following labeling with appropriate antibodies were made at least twice for each sample. TRPM4 could be detected in all 4 chambers of the heart as well as in isolated left ventricular cells. TRPM4 expression was normalized to that of α-actinin in each case. The relative expression was 0.47 ± 0.08, 0.59 ± 0.05, 0.49 ± 0.10, 0.62 ± 0.09, and 0.51 ± 0.09 in the case of tissues from the right atrium, left atrium, right ventricle, left ventricle, and isolated left ventricular cells, respectively. A significant difference could not be obtained between any of the previous samples.

4.2. The effect of CBA on the morphology of the action potential

APs were recorded under conditions of normal Ca^{2+} cycling using KCl-filled conventional microelectrodes believed to be the closest to the physiological situation. Eight cells isolated from six animals were exposed to 10 μM CBA for 5 min and a 5-min-long period of washout was applied at the end of the experiment. CBA exerted no effect on resting membrane potential (RMP), overshoot potential (OSP), membrane potential at the half duration of APD_{90} ($Plateau_{50}$), and the maximal rate of phase 3 (V^-_{max}). There was a tendency for AP shortening in the presence of CBA at all studied repolarization levels: 214.7 ± 22.3 versus 191.9 ± 18.2 ms (p = 0.09), 254.2 ± 21.2 versus 229.0 ± 17.4 ms (p = 0.07) and 266.8 ± 21.0 versus 241.1 ± 17.0 ms (p = 0.07) for APD_{50}, APD_{75}, and APD_{90}, respectively. CBA significantly reduced the maximal rates of depolarization (V^+_{max}: 133.2 ± 12.9 versus 113.1 ± 13.6 V/s). The maximal rate of early repolarization of the APs of canine left ventricular cardiomyocytes was also significantly reduced by CBA (phase-1 slope: −5.1 ± 1.2 versus −3.9 ± 1.0 V/s); however, the value of APA was increased (114.7 ± 1.8 versus 117.6 ± 1.4 mV). These changes were small but statistically significant for APA, phase-1 slope, and V^+_{max}. In case of APD_{75} and APD_{90}, statistical significance was only reached after normalizing the absolute values. APD_{75} was reduced to 91.0 ± 3.6% and APD_{90} was reduced to 91.3 ± 3.4% in the presence of CBA. Upon washout, almost all above-mentioned actions of CBA were reversible, the only exception being the maximal rate of depolarization as V^+_{max} remained 114.9 ± 10.4 V/s after washout.

4.3. Effects of CBA on Short-Term Variability of Repolarization

Analysis of short-term variability of ventricular repolarization was also determined in the same eight studied cells. APD_{90} was used to approximate the duration of cardiac APs; the values of SV and relative SV were determined according to that described in methods. The value of SV was significantly smaller, about 27% lower in CBA compared to that of the control condition (4.8 ± 0.9 ms versus 3.2 ± 0.4 ms). This decrease was mostly reversible (SV after washout: 4.2 ± 0.9 ms). The cumulative distribution curve illustrating the dispersion of differences in consecutive APD_{90} values was shifted toward smaller beat-to-beat variability in the presence of CBA in a reversible manner.

4.4. Effects of CBA Measured with a Canonic Ventricular AP Using the APVC Technique

Based on the results of the previously mentioned experiments, we wanted to be sure that CBA is selective for TRPM4, and the observed effects are not due to actions of the inhibitor evoked on ionic currents other than TRPM4. Therefore, we conducted whole cell patch-clamp recordings with an internal solution containing 10 mM BAPTA to buffer $[Ca^{2+}]_i$ and therefore prevent the activation of TRPM4 channels. The effect of BAPTA on AP morphology was observed at the beginning of each measurement to confirm its action before starting the application of CBA.

CBA-sensitive currents (I_{CBA}) were measured in five individual cells isolated from three animals. I_{CBA} possessed a short outward component during the early repolarization phase of the AP and a much longer inward component during the rest of the AP. The densities of the early outward peak current and the inward peak current were 1.38 ± 0.32 and -0.53 ± 0.06 pA/pF, respectively. The time of early outward and inward peaks measured from the peak of the AP were 2.33 ± 0.48 and 11.73 ± 0.67 ms, respectively. The effect of CBA was reversible, the I_{CBA} peak current density values after washout were significantly lower: 0.16 ± 0.06 and -0.25 ± 0.07 pA/pF, respectively. Reversibility was also observed for most AP parameters recorded with conventional microelectrodes (see above).

4.5. Effect of CBA on Ionic Currents of Repolarization

The results of the APVC experiments suggested that CBA modulates ion channels other than TRPM4. Based on the CBA-sensitive current profile, the possible targets of CBA-induced inhibition are the transient outward K^+ current (I_{to}) and the L-type Ca^{2+} current ($I_{Ca,L}$).

Therefore, to selectively study these potential candidates of CBA action, conventional voltage-clamp recordings were conducted. Just like in our APVC experiments, a BAPTA-containing internal solution was used to prevent the activation of TRPM4 channels.

I_{to} was recorded in the presence of $I_{Ca,L}$ and I_{Kr} blockade (1 μM nisoldipine and 1 μM E4031, respectively). I_{to} was activated by a 200-ms-long depolarization to +60 mV from the holding potential of −80 mV at 0.2 Hz stimulation rate. Before clamping to the test voltage, a prepulse to −40 mV was applied for 5 ms in order to activate and then inactivate the fast Na^+ current. I_{to} amplitude was measured as the difference between the peak and the pedestal of the current signal. CBA reduced I_{to} amplitude in the seven studied cells isolated from five animals by 20.4 ± 6.2% from 16.0 ± 1.8 pA/pF to 12.5 ± 1.4 pA/pF. This inhibitory effect was completely reversible (after the washout of CBA the current amplitude was 15.9 ± 2.0 pA/pF).

During $I_{Ca,L}$ recording the external Tyrode solution contained 1 μM E4031, 1 μM HMR1556, and 3 mM 4-AP to block I_{Kr}, I_{Ks}, and I_{to}, respectively. $I_{Ca,L}$ activation was achieved by 400-ms-long depolarizations to +5 mV arising from the holding potential of −80 mV at 0.2 Hz stimulation rate. The test pulse was preceded by a short (20 ms) depolarization to −40 mV to activate then inactivate the fast Na^+ current. $I_{Ca,L}$ amplitude was measured as the difference between the peak and the pedestal of the current signal. CBA had no effect on the current amplitude, which was −9.4 ± 0.6 pA/pF in control and −9.3 ± 0.8 pA/pF in the presence of CBA measured in eight cells obtained from four animals

During $I_{Na,L}$ recording, the Tyrode solution contained 1 μM nisoldipine, 100 nM dofetilide, and 100 μM chromanol-293B to eliminate any interference from Ca^{2+} and K^+ currents. Test pulses were clamped to −20 mV for 2 s from the holding potential of −120 mV at 0.2 Hz stimulation rate. The total amount of $I_{Na,L}$ was determined by pharmacological subtraction performed by a final superfusion with 20 μM TTX. The amplitude of $I_{Na,L}$ was evaluated at 50 ms after the beginning of the pulse. For determination of the current integral, the initial 20 ms was excluded from evaluation in order to minimize the contribution of peak sodium current. CBA reduced $I_{Na,L}$ in the nine studied cells isolated from five animals by 47.3 ± 7.0% from −0.70 ± 0.12 pA/pF to −0.33 ± 0.07 pA/pF. This inhibitory effect was largely reversible (after the washout of CBA, the current density was −0.56 ± 0.08 pA/pF). Similar results were obtained when the integral of $I_{Na,L}$ was determined (total charge values were −160.9 ± 36.1 mC/F, −60.0 ± 16.6 mC/F, and −117.8 ± 21.1 mC/F, in control, in the presence of CBA, and after its washout, respectively).

I_{K1} was defined as a 50 µM $BaCl_2$-sensitive current and measured with a 300 ms long ramp protocol from 0 mV to -135 mV. CBA had no effect on I_{K1} in the seven test cells obtained from the four animals (current density values of 2.09 ± 0.33 pA/pF and 2.11 ± 0.36 pA/pF measured at -50 mV in control and in the presence of CBA, respectively). After the washout of CBA, the current density was 2.29 ± 0.44 pA/pF.

4.6. 1 µM ABT-333 prolonged the left ventricular action potential

First, we perfused canine left ventricular cells with 1 µM ABT-333. During these experiments, ABT-333 perfusion lasted for 15 min, which was followed by a 20-minute-long washout. The analyzed parameters of the last ten action potentials recorded before ABT-333 perfusion were averaged to reduce the short-term variability of APs and indicated as control: bicarbonate buffer containing Tyrode solution (BTY). Again, the average of the last ten APs before the washout was considered as ABT-333, while the average of other ten APs after the 20 min washout is indicated as washout.

ABT-333 applied in 1 µM concentration, increased the AP duration of left ventricular cells from 258.3 ± 15.4 ms to 277.4 ± 15.3 ms, resulting in a 7.84 ± 3.09% increase of APD_{90}. This AP prolongation was not statistically significant ($p = 0.08$) for APD_{50}, but the prolongation tendency was reversible upon washout, just as the ABT-333-induced APD_{90} increase. ABT-333 significantly reduced the maximal rates of phase 0 and phase 1 (V_{Ph1} max) to 82.8 ± 5.1 and 51.6 ± 11.3%, respectively, in a non-reversible manner. Other AP parameters, such as the APA, the ratio of APD_{50} and APD_{90}, OSP, RMP, $Plateau_{20}$ and $Plateau_{50}$ amplitudes, and V^{-}_{max} values did not change.

4.7. Concentration Dependent Actions of ABT-333 on the Ventricular Action Potential

After detecting the 1 µM ABT-333-induced prolongation of canine left ventricular AP, we checked the actions of higher ABT-333 concentrations in a cumulative manner using 5-minute-long perfusion with increasing concentrations of ABT-333 between 1 and 30 µM. We frequently detected early afterdepolarizations (EADs) in the presence of higher ABT-333 concentrations.

ABT-333, applied in increasing concentrations, prolonged the AP of left ventricular cells, resulting in 8.1 ± 2.7, 26.3 ± 5.9, 37.6 ± 7.6, and 54.3 ± 15.2% increases in APD_{50} values in cases of 1, 3, 10, and 30 µM, respectively. Similarly, ABT-333 increased APD_{90} values by 7.4

± 2.9, 26.2 ± 6.0, 42.6 ± 8.6, and 52.6 ± 13.6% in 1, 3, 10, and 30 μM concentrations, respectively. Higher ABT-333 concentrations (3–30 μM) also increased the height of early plateau phase as $Plateau_{20}$ amplitude values were slightly, but significantly, increased by 4.3 ± 0.7, 6.1 ± 1.7, and 9.2 ± 1.2% in 3, 10, and 30 μM concentrations, respectively.

ABT-333 also reduced the maximal rate depolarization (phase 0; V^{+}_{max}), maximal rate of early repolarization (phase 1; $V_{Ph1}max$), and maximal rate of terminal repolarization (phase 3; V^{-}_{max}). Only 10 and 30 μM ABT-333 decreased V^{+}_{max} significantly to 84.4 ± 6.2 and 77.8 ± 10.9% of the control, respectively. Higher ABT-333 concentrations also reduced V^{-}_{max} values to 95.1 ± 0.9, 87.1 ± 4.2, and 84.4 ± 5.6% of the control in 3, 10, and 30 μM concentrations, respectively. ABT-333 reduced the maximal rates of phase 1 repolarization to 78.5 ± 6.3, 57.7 ± 6.8, and 40.0 ± 8.3% in the cases of 3, 10, and 30 μM, respectively.

The standard ABT-333 dose used in therapy resulted in an approximately 1 nM maximum plasma concentration in volunteers. Since the studied concentrations were an order of magnitude higher than that, we also investigated the effects of the therapeutic concentration of ABT-333 (1 nM) on action potential and showed that it has no significant effect on any parameter of AP.

4.8. Development of Early Afterdepolarizations in the Presence of ABT-333

As mentioned previously, in the presence of ABT-333, we detected EADs in certain cells. We summarized the EAD appearance in a way that EAD presence was claimed in the given cell from the lowest concentration of ABT-333 in which the first EAD appeared and in all higher concentrations, even if the EADs did not persist. We did not observe any EADs in the control, and even in the presence of 1 μM ABT-333, but in higher concentrations of the drug, the percentage of cells developing EADs gradually increased up to 70% at 30 μM ABT-333.

4.9. ABT-333-Sensitive Current Profile with AP Voltage Clamp (APVC)

ABT-333-induced AP prolongation and reduction of V^{-}_{max} suggest the inhibition of I_{Kr}, while the reduction of $V_{Ph1}max$ suggests inhibition of I_{to}. To confirm this hypothesis, we recorded the effects of 10 μM ABT-333 during the AP voltage clamp technique using a canonical AP as command potential and analyzed the properties of the ABT-333-sensitive current. The ABT-333-sensitive current was created by deducting the current trace in the presence of ABT-333 from the one recorded before ABT-333 application. Therefore, the ABT-

333-sensitive current contained all those ion currents, which was modified by ABT-333. An outward (positive) current was seen in the case of both the ABT-333-induced inhibition of an outward current as well as the ABT-333-induced increase in an inward current.

The 10 μM ABT-333-sensitive current was outward throughout the AP. We observed an early outward current peak with a density of 2.76 ± 0.64 pA/pF measured at 2.90 ± 0.81 ms later than the time of the V_{Ph1} max of the command AP. On the basis of the shape of the own AP of the studied cells, there was a negative correlation between the V_{Ph1}max values and the early outward peak current density values. The outward current at the half duration of the command AP was 0.89 ± 0.24 pA/pF. The end of the sustained outward current (I_{endsus}, measured just before the start of returning to zero) was 0.83 ± 0.16 pA/pF, and its position was 7.82 ± 1.64 ms before the time of the V^{-}_{max} of the canonical AP. There was no correlation between the density of I_{endsus} and the V^{-}_{max} values of the own AP of the measured cells.

4.10. ABT-333 Blocked Expressed hERG Channels in a Time- and Concentration-Dependent Manner

ABT-333 inhibited the hERG current in 30 μM concentration as observed by a 3-second-long depolarizing step to +20 mV followed by a repolarizing step to −40 mV, which led to a characteristic fast recovery of inactivated hERG channels. The holding potential was −80 mV, and pulses were applied every 30 s. The application of ABT-333 caused a reduction of the hERG current both at +20 and −40 mV. The monotonic increasing control current at +20 mV changed into a decaying current in the presence of ABT-333, which was fit with a single exponential function, yielding a time constant of 0.87 ± 0.09 s. To test the concentration dependence of the inhibition, we applied 1, 3, 10, and 30 μM ABT-333. The remaining current fractions (RCFs) were 0.93 ± 0.04, 0.63 ± 0.05, 0.26 ± 0.04, and 0.15 ± 0.02, respectively ($n \geq 4$ for each concentration). The concentration–response curve yielded a half maximal inhibitory concentration (IC_{50}) of 3.2 μM. The effect of ABT-333 on the voltage sensing of hERG channels was tested by an I-V protocol consisting of depolarizing pulses ranging from −50 mV to +50 mV in +10 mV increments. From the normalized tail current peaks, we created the G-V curves of the control solution and the 30 μM ABT-333-superfused recordings. Fitting them with the Boltzmann equation, the $V_{1/2}$ value for the control solution was 6.50 ± 1.03 mV. For ABT-333, the $V_{1/2}$ value could not be obtained this way due to the too small current. However, visually, a large voltage-shift was not apparent.

Since ABT-333 caused time-dependent inhibition (time constant 0.87 ± 0.09 s), we investigated the possible effects of ABT-333 on the gating transitions of the hERG channel. ABT-333 at concentrations as low as 3 μM significantly reduced the deactivation time constant ratio ($\tau_{ABT\text{-}333}$ / $\tau_{Control}$ = 0.46 ± 0.04, p = 0.0001), and perfusion of 30 μM ABT-333 reduced the inactivation time constant ratio to 0.78 ± 0.15. These results suggest that ABT-333 blocks the channel pore mainly in the open state.

5. Discussion

5.1. TRPM4 Expression in the Canine Heart

TRPM4 is abundantly expressed in many tissues, including the heart, but our group has shown for the first time that it is expressed in healthy canine hearts. Although we could not detect significant differences in TRPM4 expression between samples obtained from the walls of four different chambers of the canine heart, previously, a six-times-higher expression was reported in the right ventricle compared to that of the left in the rat. Although cardiomyocytes account for the vast majority of cells in cardiac tissue, excised samples also contain other cell types, including fibroblasts, smooth muscle, and endothelial cells. To minimize the interference of other cell types, the expression of TRPM4 was also determined directly on enzymatically isolated left ventricular cells. There was no significant difference in TRPM4 expression between isolated cells of the left ventricle and whole left ventricular wall tissue, suggesting that the source of the TRPM4 signal is mostly from cardiomyocytes. Our results are in agreement with a recent study where equal TRPM4 expression was shown in mice atrial and ventricular samples, and in isolated ventricular cardiomyocytes.

5.2. Effects of CBA on Action Potential Morphology

For AP measurements, the conventional sharp microelectrode technique was used to study the effect of the TRPM4 inhibitor CBA on canine left ventricular myocytes. This technique best approximates the physiological state because it does not affect the composition of the intracellular space of the cells under study.

In the present study, CBA was used at 10 µM, where a previous study reported at least 90% inhibition of TRPM4 current, but no significant effect on either hERG or L-type calcium channels was observed. This is the first report where the effect of CBA was studied in native cardiac cells—all previous studies were using either TRPM4 knockout animals or other TRPM inhibitors like 9-phenanthrol.

Our results indicate that CBA reduced phase-1 slope and increased the action potential amplitude in a reversible manner. The CBA-induced reduction in maximal rate of depolarization, however, could not be reversed. There was only a tendency for AP shortening but after normalization of the APD_{90} values, to those recorded under control conditions, it resulted in a small (approximately 9%) but significant decrease. These changes can occur due

to either CBA-mediated TRPM4 inhibition or nonspecific actions of CBA evoked on ion channels other than TRPM4, or a combination of these. To hypothesize possible electrophysiological changes caused by TRPM4 inhibition, we need to imagine what the TRPM4-mediated current might look like during ventricular AP. To do this, we need to consider the Ca^{2+}-dependent activation of TRPM4 and its selectivity for monovalent cations. In ventricular cells, membrane potential and intracellular Ca^{2+} concentration also change dynamically during the cardiac cycle. In addition, Ca^{2+} concentrations differ significantly in various cellular compartments. The peak Ca^{2+} concentrations can rise to approximately 600 nM in the cytoplasm, up to 6 µM in the subsarcolemmal space, and up to 10-50 µM in the submembrane cleft (the narrow space between the sarcolemmal Ca^{2+} entry and sarcoplasmic reticulum Ca^{2+} release sites). Regarding the Ca^{2+} concentration required for TRPM4 activation, the EC_{50} values are quite variable in the literature, starting from as low as 400 nM and reaching to as high as 1 mM, depending on the experimental conditions. In native sinoatrial and ventricular cardiomyocytes, the minimal Ca^{2+} concentration for channel activation was between 0.1–1 µM and the EC_{50} was 10 µM in rat ventricular cells. Based on these, it is likely that TRPM4 can indeed be activated during the cardiac action potential by the Ca^{2+} influx and the consequent Ca^{2+} release. The highest activation is expected shortly after the AP peak and during the early plateau phase, because the peak calcium concentration is reached within a few ms after the AP peak in the subsarcolemmal space, and even faster in the submembrane cleft. Based on the fact that TRPM4 is permeable to both Na^+ and K^+ (but not to Ca^{2+}), the expected reversal potential of its current is around 0 mV. According to these, TRPM4 activation is expected to force the membrane potential towards 0 mV, resulting in a repolarizing current right after the AP peak. Therefore, upon CBA-induced TRPM4 inhibition, the slowing of phase-1 repolarization is anticipated, as seen in our experiments.

The TRPM4-mediated current, on the other hand, could reduce the plateau potential in the early plateau phase, when the membrane potential is higher than 0 mV. Theoretically, the more positive the membrane potential, the larger this reduction will be. Additionally, it might elevate the potential of the late plateau, if the current is still active at this time, but based on the fast decay of calcium levels in the vicinity of the TRPM4 channels, this is quite unlikely. Therefore, TRPM4 blockade by CBA is expected to somewhat elevate the potential of the early plateau and maybe to very moderately reduce the membrane potential of the late plateau. In our experiments, the plateau potential was not significantly altered by CBA

(despite the approximately 2 mV increase of the initially slightly positive $Plateau_{50}$ potential). This can be explained by (1) the nearly 0 value of the $Plateau_{50}$ or (2) it suggests either the insufficient Ca^{2+} level for TRPM4 activation at this later phase of the AP or (3) actions of CBA on channels other than TRPM4, being active during that phase.

In theory, a shortening of AP duration is expected from TRPM4 inhibition as observed in rabbit Purkinje fibers in the presence of a different TRPM4 blocker (30 μM 9-phenanthrol) and in murine atrial cells lacking TRPM4. Our results are similar to these, but only a tendency for APD_{90} reduction was observed (approximately 25 ms) and that was only significant after normalization to the initial APD_{90} values of each studied cell, resulting in 9% APD_{90} reduction. In rabbit ventricular cells, TRPM4 inhibition by 30 μM 9-phenanthrol was, however, without effect on AP amplitude and duration as well as on resting membrane potential and V^{+}_{max}.

The action of CBA on AP amplitude was statistically significant but very small (3 mV or 2.5% increase) and might be due to the sum of the non-significant increase and decrease of overshoot potential and resting membrane potential, respectively. From the TRPM4 inhibition during the AP peak, this can be expected, as TRPM4 would tend to move the membrane potential towards 0 mV, therefore antagonizing depolarization, which effect is reduced by CBA, resulting in the increase of overshoot potential and/or AP amplitude. Regarding the maximal rate of depolarization, its CBA-induced reduction might be due to the inhibition of fast Na^{+} current, as V^{+}_{max} is a fairly good measure of those channels. However, the relationship between V^{+}_{max} and sodium current density is not linear; therefore, a small change in V^{+}_{max} can be due to a larger decrease of fast Na^{+} current. The CBA-induced irreversible V^{+}_{max} reduction was about 15% but not observed in murine ventricular myocardium. A recent study, however, described the smaller value of V^{+}_{max} in ventricular myocytes of TRPM4 knockout mice compared to that in wild-type animals. The smaller V^{+}_{max} value was due to the reduction of peak Na^{+} current density as it was approximately 30% smaller in TRPM4 knockout mice. It might be that the CBA-induced reduction of V^{+}_{max} in our study reflects the reduction peak Na^{+} current, as TRPM4 and Nav1.5 were shown to interact with each other. Our previous results obtained with 9-phenanthrol are in good agreement with the current result regarding the V^{+}_{max} and phase-1 slope as both drugs reduced both parameters. In contrast, CBA had no action on either $Plateau_{50}$ or V^{-}_{max}, unlike the reduction of these by 30 μM 9-phenanthrol. Similarly, the actions of CBA and 9-phenanthrol were different on APD_{90} as a shortening tendency was seen with CBA, but APD reduction was the case in only the

minority of the cells with 10 and 30 μM 9-phenanthrol and the prolongation of AP was seen on average. It seems, therefore, that despite the similar TRPM4 inhibition of CBA and 9-phenanthrol, their effects on the canine ventricular AP configuration are markedly different. This is likely due to their different actions on other, non-TRPM4 channels.

5.3. Effects of CBA on Short-Term Variability of Repolarization

TRPM4 channels can mediate transient inward current (like calcium-activated chloride and sodium-calcium exchange currents), leading to delayed afterdepolarizations (DADs) in calcium-overloaded cells. These can lead to cardiac arrhythmias by initiating Torsade de Pointes type malignant ventricular tachyarrhytmia.

We studied the CBA-induced TRPM4 inhibition of short-term variability of repolarization (SV), a good predictor of cardiac arrhythmias. Since reduction of SV may have antiarrhythmic properties, TRPM4 appears to have a pro-arrhythmic effect, as its inhibition by CBA caused a reversible reduction in SV. A large, sudden change in consecutive APD values (especially if that happens in a non-uniform manner of the myocardium), can more effectively induce an arrhythmic event. Therefore, in order to detect any unusually short or long APs, consecutive APD values were binned and the overall probability of their appearances was plotted. The curve was reversibly shifted to the left, supporting again the reduction of chance of cardiac arrhythmia in the presence of CBA. Based on these, it seems that the native TRPM4 current might contribute to cardiac arrhythmia, in agreement with previous studies. Our results, however, suggest a mechanism based on TRPM4 current mediated increase in SV, rather than EAD induction as it was shown previously. It must be mentioned that as CBA might interfere with other ion currents (discussed later), and those could also contribute to the overall effect of CBA on SV as well as on relative SV. Therefore, the reduction of SV might partially be due to the CBA-induced reduction of I_{to} and $I_{Na,L}$, as those two currents are likely to increase SV and parallelly, the role of the TRPM4-mediated current in SV increase might be smaller. Since these changes could also be due to the effects of CBA on non-TRPM4 ion channels, we tested this possibility using conventional voltage-clamp measurements.

5.4. Effects of CBA Measured with APVC and Conventional Voltage Clamp

As well as the direct inhibition of TRPM4 channels, CBA-induced changes in AP morphology can also be caused by nonspecific actions of the compound. For instance, the

reduction of V^{+}_{max} can be due to inhibition of Na^{+} channels, reduction of phase-1 slope, and the increase of APA might be the result of I_{to} inhibition, and the tendency for AP shortening might be due to inhibition of $I_{Na,L}$ or $I_{Ca,L}$ or in theory activation of late K^{+} currents (I_{Kr}, I_{Ks}, possibly I_{K1}). To exclude the possibility of CBA action on ion channels other than TRPM4, we used the whole cell configuration of patch-clamp technique where we applied the fast calcium chelator BAPTA in 10 mM to prevent the activation on TRPM4. This BAPTA concentration is able to fully eliminate not just the intracellular Ca^{2+} transient but also to prevent the systolic rise of subsarcolemmal and probably the submembrane cleft Ca^{2+} levels. Indeed, at least in arterial smooth muscle, 10 mM BAPTA was shown to reduce Ca^{2+} levels in microdomains, therefore preventing the activation of TRPM4. Although not done on direct TRPM4 current recordings, other studies also suggest that BAPTA can block TRPM4. Obviously, it has to be mentioned that the application of BAPTA not only prevents the activation of TRPM4 but also influences all Ca^{2+} sensitive currents including L-type Ca^{2+} current (where its Ca^{2+}-dependent inactivation is lost, leading to a higher current), Ca^{2+}-activated Cl^{-} current (where its activation is prevented), I_{Ks} (where its otherwise small activation during a normal duration AP is probably further reduced), and I_{NCX} (which will operate in reverse mode, resulting in Ca^{2+} entry leading to an outward current). These will certainly modify the shape of the AP, but during our measurements, the same canonic APs were always used to stimulate the cells. Actually, the blockade of the Ca^{2+}-activated Cl^{-} current and the reduction of the already quite small I_{Ks} were beneficial as CBA were not able to modify those in case of the 10 mM BAPTA-containing AP voltage clamp experiments. During conventional voltage protocols, we isolated the studied currents one-by-one using specific inhibitors and voltage pulses and studied the possible influence of CBA on the given current.

As mentioned before, CBA was only applied after confirming the action of BAPTA on AP contour. The early short outward peak of the CBA-sensitive current could be due to CBA induced inhibition of transient outward current flowing during phase-1. As the activation of the calcium activated chloride current was prevented with 10 mM BAPTA, the inhibited current can only be the transient outward K^{+} current. Indeed, we confirmed this with conventional voltage clamp protocol where all other major currents were either blocked by inhibitors (nisoldipine and E4031) or inactivated by a voltage prepulse. The reversible reduction of I_{to} can account for the outward component of CBA-sensitive current of APVC

experiments and also fits well with the CBA induced reduction of phase-1 slope and the slight increase of AP amplitude. The long inward current seen in CBA sensitive current might be due to reduction of L-type Ca^{2+} or late sodium current. CBA induced I_{NCX} inhibition is unlikely in our conditions of heavy Ca^{2+} buffering, where that current is mainly outward. CBA had no effect on L-type Ca^{2+} current in agreement with a previous study. Late sodium current however was reduced by CBA, which can contribute to the small reduction of AP duration seen with AP measurements. As mentioned before a smaller Na^{+} current peak was observed in TRPM4 knockout mice but the late sodium current was not recorded. Nevertheless, it is possible that the late sodium current might also be larger in the presence of TRPM4.

From our results, it is unlikely that CBA interferes with the delayed rectifier K^{+} currents shaping the AP: I_{Kr} and I_{Ks}, as the inhibition of these would result in outward currents during the plateau phase of AP measured with APVC. Moreover, if these currents were reduced by CBA the prolongation of the AP could be expected. I_{K1} also plays an important role in terminal repolarization, but we excluded its CBA sensitivity which is in agreement with no change in the RMP and V^{-}_{max} seen in AP measurements. In addition, during APVC experiments where TRPM4 could not be activated it would be even more likely to observe these nonspecific inhibitory effects of CBA. Again, on the CBA sensitive current traces neither diastolic current (characteristic marker of I_{K1} blockade) or outward current increasing or reaching peak towards the end of the AP (characteristic marker of I_{Kr} and I_{K1} inhibition) could be observed. As neither AP changes nor the CBA sensitive current suggested potential inhibition of I_{K1}, I_{Kr} and I_{Ks} we can rule out the CBA inhibition of these three K^{+} currents even in the absence of direct current measurements in case of I_{Kr} and I_{Ks}. The lack of CBA action on I_{Kr} could be expected as cardiac hERG channels (the pore forming subunit of I_{Kr}) were not influenced by CBA as less than 5% reduction was detected by 10 μM CBA judged by reduction in specific antagonist (dofetilide) binding.

5.5. Effects of 1 μM ABT-333

We first tested ABT-333 actions on cardiac AP in 1 μM, where APD_{90} was significantly and reversibly increased, likely due to the expected I_{Kr} blockade of the drug. I_{Kr} is responsible for the initiation of phase 3 repolarization, but its maximal rate (the value of V^{-}_{max}) mainly but not exclusively depend on the density of inward rectifier potassium current, I_{K1}.

Accordingly, ABT-333 did not reduce V^{-}_{max} in 1 μM concentration, suggesting that it did

not inhibit I_{K1}. The APD_{50}/APD_{90} ratio is often used as a marker of AP triangulation. The smaller the value, the more triangular the shape of the cardiac APs, which is often seen during inhibition of I_{K1}. As the APD_{50}/APD_{90} ratio did not change significantly in the presence of ABT-333, it also confirms that the drug did not inhibit I_{K1}.

The ABT-333-induced V_{Ph1}max and V^{+}_{max} reductions can be caused by the inhibition of I_{to} and I_{Na}, respectively. These actions did not reverse the 20 min washout, raising the possibility of an irreversible channel blockade by ABT-333.

5.6. Actions of Higher Concentrations of ABT-333

Compared to 1 μM ABT-333, higher concentrations of the drug generated further changes of AP parameters. Both APD_{50} and APD_{90} values, as well as the amplitude of early plateau phase ($Plateau_{20}$ amplitude), were increased in a concentration-dependent manner, suggesting again that ABT-333 reduced I_{Kr}.

V^{+}_{max} and V_{Ph1}max values were also smaller in the presence of ABT-333. These observations raise the possibility of I_{to} and I_{Na} inhibition apart from I_{Kr} blockade.

At larger concentrations of ABT-333, EADs appeared, also suggesting the inhibition of I_{Kr}, as AP prolongation often leads to EAD formation. In a computer simulation study, major (more than 90%) I_{Kr} reduction was needed for EAD development. The APD increase, however, is not always due to I_{Kr} inhibition but can be due to the increase in sodium or calcium currents. The former one can probably be ruled out as the reduction of V^{+}_{max} seen with ABT-333 is not consistent with a larger sodium current. Calcium current increase by ABT-333 is a possibility, especially as it would lead to elevation of the early plateau potential, which was indeed detected with ABT-333. Therefore, it is possible that ABT-333 greatly reduced I_{Kr} or induced EADs by reduction of I_{Kr} and simultaneous increase in the calcium current, especially in higher concentrations.

5.7. ABT-333-Sensitive Current Profile with APVC

ABT-333-induced reduction of V_{Ph1}max suggested inhibition of I_{to} on top of the I_{Kr} inhibition. We tried to confirm this with the APVC measurements. The properties of the early outward peak of the average ABT-333-sensitive current were very similar to that shown earlier with the I_{to} inhibitor 4-AP. It was found that 1 mM 4-AP inhibits approximately 70% of I_{to} and resulted in approximately 3 pA/pF peak current density. The ABT-333-sensitive current

early peak density was slightly smaller: 2.76 ± 0.64 pA/pF, probably due to the higher presence of cells with small I_{to} current in the current study. Moreover, the time of the ABT-333-sensitive current peak was always after the time of V_{Ph1}max but before the deepest point of the incisura of the command potential. Further proof that ABT-333 reduces I_{to} is the good correlation between early current peak density values and V_{Ph1}max values of own APs. Moreover, the early outward current decayed very rapidly, similarly to the 4-AP-sensitive current. An amount of 100 µM chromanol 293B can also be used to study I_{to}, wherein the decay of the current was less rapid. Of note, the ABT-333-sensitive current did not decay to nearly zero, as seen with the 4-AP-sensitive one. This might have been due to the effect of ABT-333 on other ion channels conducting during this early plateau phase of the AP. Nevertheless, on the basis of the results, it seems that 10 µM ABT-333 inhibits I_{to} substantially.

The inhibitory effect expected from ABT-333 I_{Kr} was also confirmed with APVC. The position of I_{endsus} was 7.82 ± 1.64 ms before the time of V^{-}_{max} of command potential, which is in good agreement with earlier results. The peak value of the 1 µM E4031-sensitive current was approximately 0.6 pA/pF, slightly smaller than the ABT-333-sensitive current of the current study (approx. 0.8 pA/pF). This could have been due to larger I_{Kr} currents in cells of the current study than those in our previous one as 1 µM E4031 inhibits approximately 80% of I_{Kr}, similarly to the large reduction of hERG by 10 µM ABT-333. In addition, it is possible that ABT-333-sensitive current might contain an activated calcium current component besides I_{to} and I_{Kr}, as suggested previously. This activated calcium current, if still active during the late phase of plateau, can add to the late peak value of the ABT-333-sensitive current on top of the I_{Kr}, resulting in a larger last part than the E4031 sensitive current. This possibility is evident if one observes the fingerprints of I_{to} and I_{Kr}, as I_{to} decays to zero at the latest after 50 ms of the AP peak, while I_{Kr} only starts to activate about 70–80 ms after the AP peak. However, I_{to} can decay more slowly and therefore might contribute to the maintained outward component of the ABT-333-sensitive current during the early plateau phase. The ABT-333-induced augmentation of late sodium or calcium current can be also responsible, as that will appear as an outward current. The contribution of the late sodium current is, however, unlikely, as ABT-333 reduced the V^{+}_{max} value of the AP, which argues against sodium current activation.

5.8. ABT-333-Induced Reduction of hERG Channel Currents

ABT-333-induced AP parameter changes, namely, the increase in APD_{50} and APD_{90}, mainly without the alteration of their ratio; the reduction of V^{-}_{max}, suggested the inhibition of I_{Kr}. This was expected due to the presence of the methanesulfonamide group in the structure of ABT-333. Moreover, the ABT-333-sensitive current was also outward during the late plateau phase, suggesting I_{Kr} inhibition as well. To confirm this, we carried out experiments on HEK cells stably expressing hERG channels. The hERG-mediated current was indeed reduced by ABT-333 in a concentration-dependent manner with an IC_{50} of 3.2 µM. Similarly, to some AP parameters where ABT-333-induced changes were (partly) irreversible upon washout, the reduction of hERG current by ABT-333 also was unable to be fully reversed. Moreover, applying ABT-333 in 30 µM concentration caused the time-dependent inhibition during the depolarizing pulse with a time constant of 0.87 ± 0.09 s. This led us to investigate the possible effects of the ABT-333 on the hERG channel gating transitions. On this basis, 3 µM ABT-333 significantly decreased the deactivation time constant ratio ($\tau_{ABT\text{-}333}/\tau_{Control}$ = 0.46 ± 0.04), and the superfusion of 30 µM ABT-333 decreased the inactivation time constant ratio to 0.78 ± 0.15. These results suggest that ABT-333 blocks the channel pore mainly during the open state of the channel.

5.9. Medical relevance

According to our hypothesis, ABT-333 indeed blocked the I_{Kr} current. This was supported by (1) prolongation of canine ventricular AP; (2) reduction of V^{-}_{max}; (3) detecting I_{Kr}-like profile of the late phase of the ABT-333-sensitive current with APVC; and (4) inhibition the current of expressed hERG channels, the pore forming protein responsible for I_{Kr}. In this study, we used ABT-333 between 1-30 µM, but given the large difference between the therapeutic dose of ABT-333 (1 nM), we also tested the therapeutic concentration of ABT-333. Our results suggest that the therapeutic dose is safe and that ABT-333 does not significantly affect any of the left ventricular AP parameters.

6. Summary

6.1. CBA - TRPM4

TRPM4 protein expression was detected in the wall of all four chambers of the canine heart and in isolated left ventricular canine cardiomyocytes. CBA is a rather new TRPM4 inhibitor more specific than 9-phenanthrol, and thus more suitable for studying the role of TRPM4 in cardiac physiology.

CBA decreased the slope of phase-1 repolarization and slightly increased AP amplitude, effects probably due to the inhibitory effect of agent on I_{to}. The tendency of AP shortening can be explained by inhibition of inward currents seen in APVC measurements in the plateau phase. This effect is probably due to the inhibitory effect of CBA on inward $I_{Na,L}$ currents.

Our results suggest that CBA is not fully selective for TRPM4 channels and therefore cannot be used alone in native tissue for functional assessment of the channel, and that its use in pharmacological combination requires increased caution.

6.2. ABT-333 - I_{Kr} (hERG)

Based on its molecular structure, ABT-333 potentially blocks hERG channels and I_{Kr} current. Application of 1 µM ABT-333 reversibly prolonged the AP. The maximum velocity of phases 0 and 1 showed an irreversible decrease. Higher concentrations of ABT-333 caused greater AP prolongation, an increase in early plateau potential, and a decrease in the maximum rates of phases 0, 1 and 3. EADs appeared in some cells when ABT-333 at concentrations of 3-30 µM was applied.

The 10 µM ABT-333-sensitive current measured by the APVC technique contained a late outward component identifiable as I_{Kr}, and an early outward component identifiable as I_{to}. ABT-333 reduced the ionic current mediated by the hERG channel in a concentration-dependent, partially reversible manner, with a half-inhibitory concentration of 3.2 µM.

Despite all these, ABT-333 is considered safe for cardiac arrhythmias, as its plasma levels do not reach high concentrations even in the case of overdose and its therapeutic concentration has no action on the AP.

UNIVERSITY AND NATIONAL LIBRARY
UNIVERSITY OF DEBRECEN
H-4002 Egyetem tér 1, Debrecen
Phone: +3652/410-443, email: publikaciok@lib.unideb.hu

Registry number: DEENK/532/2023.PL
Subject: PhD Publication List

Candidate: Csaba Dienes
Doctoral School: Doctoral School of Molecular Medicine
MTMT ID: 10068161

List of publications related to the dissertation

1. Kovács, Z. M., Óvári, J., **Dienes, C.**, Magyar, J., Bányász, T., Nánási, P. P., Horváth, B., Fehér, Á., Varga, Z., Szentandrássy, N.: ABT-333 (Dasabuvir) Increases Action Potential Duration and Provokes Early Afterdepolarizations in Canine Left Ventricular Cells via Inhibition of IKr. *Pharmaceuticals (Basel). 16* (4), 1-18, 2023.
   DOI: http://dx.doi.org/10.3390/ph16040488
   IF: 4.6 (2022)

2. **Dienes, C.**, Hézső, T., Kiss, D. Z., Baranyai, D., Kovács, Z. M., Szabó, L., Magyar, J., Bányász, T., Nánási, P. P., Horváth, B., Gönczi, M., Szentandrássy, N.: Electrophysiological Effects of the Transient Receptor Potential Melastatin 4 Channel Inhibitor (4-Chloro-2-(2-chlorophenoxy)acetamido) Benzoic Acid (CBA) in Canine Left Ventricular Cardiomyocytes. *Int. J. Mol. Sci. 22* (17), 9499, 2021.
   DOI: http://dx.doi.org/10.3390/ijms22179499
   IF: 6.208

List of other publications

3. Horváth, B., Kovács, Z. M., **Dienes, C.**, Óvári, J., Szentandrássy, N., Magyar, J., Bányász, T., Varró, A., Nánási, P. P.: Conductance Changes of Na+ Channels during the Late Na+ Current Flowing under Action Potential Voltage Clamp Conditions in Canine, Rabbit, and Guinea Pig Ventricular Myocytes. *Pharmaceuticals (Basel). 16* (4), 1-14, 2023.
   DOI: http://dx.doi.org/10.3390/ph16040560
   IF: 4.6 (2022)

UNIVERSITY of DEBRECEN

UNIVERSITY AND NATIONAL LIBRARY
UNIVERSITY OF DEBRECEN
H-4002 Egyetem tér 1, Debrecen
Phone: +3652/410-443, email: publikaciok@lib.unideb.hu

4. Naveed, M., Mohammed, A. S. A., Topal, L., Kovács, Z. M., **Dienes, C.**, Óvári, J., Szentandrássy, N., Magyar, J., Bányász, T., Prorok, J., Jost, N., Virág, L., Baczkó, I., Varró, A., Nánási, P. P., Horváth, B.: Selective Inhibition of Cardiac Late Na+ Current Is Based on Fast Offset Kinetics of the Inhibitor.
Biomedicines. 11 (9), 2383, 2023.
DOI: http://dx.doi.org/10.3390/biomedicines11092383
IF: 4.7 (2022)

5. Horváth, B., Szentandrássy, N., **Dienes, C.**, Kovács, Z. M., Nánási, P. P., Chen-Izu, Y., Izu, L. T., Bányász, T.: Exploring the Coordination of Cardiac Ion Channels With Action Potential Clamp Technique.
Front. Physiol. 13, 864002, 2022.
DOI: http://dx.doi.org/10.3389/fphys.2022.864002
IF: 4

6. Horváth, B., Szentandrássy, N., Almássy, J., **Dienes, C.**, Kovács, Z. M., Nánási, P. P., Bányász, T.: Late Sodium Current of the Heart: where Do We Stand and Where Are We Going?
Pharmaceuticals (Basel). 15 (2), 231, 2022.
DOI: http://dx.doi.org/10.3390/ph15020231
IF: 4.6

7. Kovács, Z. M., **Dienes, C.**, Hézső, T., Almássy, J., Magyar, J., Bányász, T., Nánási, P. P., Horváth, B., Szentandrássy, N.: Pharmacological Modulation and (Patho)Physiological Roles of TRPM4 Channel-Part 1: modulation of TRPM4.
Pharmaceuticals (Basel). 15 (1), 81, 2022.
DOI: http://dx.doi.org/10.3390/ph15010081
IF: 4.6

8. **Dienes, C.**, Kovács, Z. M., Hézső, T., Almássy, J., Magyar, J., Bányász, T., Nánási, P. P., Horváth, B., Szentandrássy, N.: Pharmacological Modulation and (Patho)Physiological Roles of TRPM4 Channel-Part 2: TRPM4 in Health and Disease.
Pharmaceuticals (Basel). 15 (1), 40, 2022.
DOI: http://dx.doi.org/10.3390/ph15010040
IF: 4.6

9. Horváth, B., Kiss, D. Z., **Dienes, C.**, Hézső, T., Kovács, Z. M., Szentandrássy, N., Almássy, J., Magyar, J., Bányász, T., Nánási, P. P.: Ion current profiles in canine ventricular myocytes obtained by the "onion peeling" technique.
J. Mol. Cell. Cardiol. 158, 153-162, 2021.
DOI: http://dx.doi.org/10.1016/j.yjmcc.2021.05.011
IF: 5.763

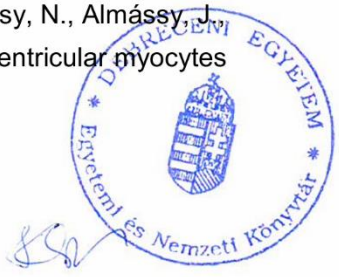

UNIVERSITY of DEBRECEN

UNIVERSITY AND NATIONAL LIBRARY
UNIVERSITY OF DEBRECEN
H-4002 Egyetem tér 1, Debrecen
Phone: +3652/410-443, email: publikaciok@lib.unideb.hu

10. Kiss, D. Z., Horváth, B., Hézső, T., **Dienes, C.**, Kovács, Z. M., Topal, L., Szentandrássy, N., Almássy, J., Prorok, J., Virág, L., Bányász, T., Varró, A., Nánási, P. P., Magyar, J.: Late Na+ Current Is [Ca2+]i-Dependent in Canine Ventricular Myocytes.
Pharmaceuticals (Basel). 14 (11), 1142, 2021.
DOI: http://dx.doi.org/10.3390/ph14111142
IF: 5.215

11. Hézső, T., Naveed, M., **Dienes, C.**, Kiss, D. Z., Prorok, J., Árpádffy-Lovas, T., Varga, R., Fujii, E., Mercan, T., Topal, L., Kistamás, K., Szentandrássy, N., Almássy, J., Jost, N., Magyar, J., Bányász, T., Baczkó, I., Varró, A., Nánási, P. P., Virág, L., Horváth, B.: Mexiletine-like cellular electrophysiological effects of GS967 in canine ventricular myocardium.
Sci. Rep. 11, 9565, 2021.
DOI: http://dx.doi.org/10.1038/s41598-021-88903-3
IF: 4.996

12. Horváth, B., Hézső, T., Szentandrássy, N., Kistamás, K., Árpádffy-Lovas, T., Varga, R., Gazdag, P., Veress, R., **Dienes, C.**, Baranyai, D., Almássy, J., Virág, L., Nagy, N., Baczkó, I., Magyar, J., Bányász, T., Varró, A., Nánási, P. P.: Late sodium current in human, canine and guinea pig ventricular myocardium.
J. Mol. Cell. Cardiol. 139, 14-23, 2020.
DOI: http://dx.doi.org/10.1016/j.yjmcc.2019.12.015
IF: 5

13. Veress, R., Baranyai, D., Hegyi, B., Kistamás, K., **Dienes, C.**, Magyar, J., Bányász, T., Nánási, P. P., Szentandrássy, N., Horváth, B.: Transient receptor potential melastatin 4 channel inhibitor 9-phenanthrol inhibits K+ but not Ca2+ currents in canine ventricular myocytes.
Can. J. Physiol. Pharmacol. 96 (10), 1022-1029, 2018.
DOI: http://dx.doi.org/10.1139/cjpp-2018-0049
IF: 2.041

Total IF of journals (all publications): 60,923
Total IF of journals (publications related to the dissertation): 10,808

The Candidate's publication data submitted to the iDEa Tudóstér have been validated by DEENK on the basis of the Journal Citation Report (Impact Factor) database.

DEBRECENI EGYETEM * Egyetemi és Nemzeti Könyvtár *

05 December, 2023